A Simultaneous Multiband Continuous-Time ΔΣ ADC With 90-MHz Aggregate Bandwidth in 40-nm CMOS

John Bell, *Student Member, IEEE*, and Michael P. Flynn, *Fellow, IEEE*

***Abstract*—This letter presents a new class of ΔΣ modulator that combines any set of traditional NTF shapes in a single modulator. The prototype multiband ΔΣ modulator (MB-ΔΣM) demonstrates two simultaneous bands—one baseband and one bandpass. These two bands are separated by 500 MHz, have an aggregate bandwidth of 90 MHz, with up to 55-dB measured SNDR. In addition to reducing the number of ADCs, this new approach promises further system-level power savings by simplifying the RF frontend. The system-level power savings from requiring fewer analog mixers, LNAs, filters, and ADC drivers can be even more than the ADC power reduction.**

***Index Terms*—Carrier aggregation, continuous-time delta-sigma modulation, delta-sigma modulation, filter synthesis, multiband delta-sigma modulation.**

I. Introduction

To keep up with increasing bandwidth demands, carrier aggregation (CA) has become an essential part of LTE-A and emerging 5G standards. While intraband CA is approachable with current technology, interband CA is far more difficult to accomplish efficiently, due to the large band separations of 100's of MHz required. Conventional approaches to this problem simply use parallel receivers [1] [Fig. 1(a)] or digitize a wide spectrum range encompassing all bands of interest [2] [Fig. 1(b)]. However, both of these approaches are power-hungry and area-intensive. The CT-ΔΣ ADC is a popular choice for wireless transceivers, because of its resistive input and anti-aliasing properties. We introduce the multiband CT-ΔΣ ADC to simultaneously and efficiently digitize only the bands of interest [Fig. 1(c)].

In addition to reducing the number of ADCs, our multiband ADC approach alleviates the need for multiple power-hungry front ends. By only driving one ADC, we remove mixers, buffers, and LNAs, since each of the bands-of-interest do not need to be separated before the ADC. Instead, we efficiently separate the bands as a natural part of the ADC's existing digital decimation filtering. Using [1] as an example, the power consumed per band by a parallel front end can be as high as 72 mW; removing one channel saves 60% more power than the multiband ADC itself.

The approach improves on a single wide-band ADC [Fig. 1(b)] by making much more efficient use of the ΔΣ noise-shaping spectrum. This allows a much lower clock rate, leading to significant overall power savings—nearly 900 mW, in the case of [2]. Lastly, even though [2] has the widest BW of any CMOS ΔΣ to-date, it is still not wide enough to capture the 500 MHz band separation used in this letter.

We present the first multiband ΔΣ modulator (MB-ΔΣM). The multiband ΔΣ suppresses quantization noise only in the bands of interest. To enable this new architecture, we also introduce: 1) a feed-forward (FF) synthesis method which simplifies implementation of the high-order loop filter; 2) a modified single-amplifier biquad which simplifies the DAC design; and 3) a modification to the input resistor network that reduces loop filter nonlinearity and interband distortion. The prototype multiband CT-ΔΣ simultaneously digitizes two bands—one at baseband (BB) and one at 500 MHz—delivering an aggregate bandwidth of 90 MHz.

Manuscript received June 22, 2019; revised July 27, 2019; accepted July 31, 2019. Date of publication October 15, 2019; date of current version October 15, 2019. This article was approved by Associate Editor Georges Gielen. This work was supported by the Semiconductor Research Corporation. *(Corresponding author: John Bell.)*

The authors are with the Department of Electrical Engineering, University of Michigan, Ann Arbor, MI 48109 USA (e-mail: johnlb@umich.edu).

Digital Object Identifier 10.1109/LSSC.2019.2933159

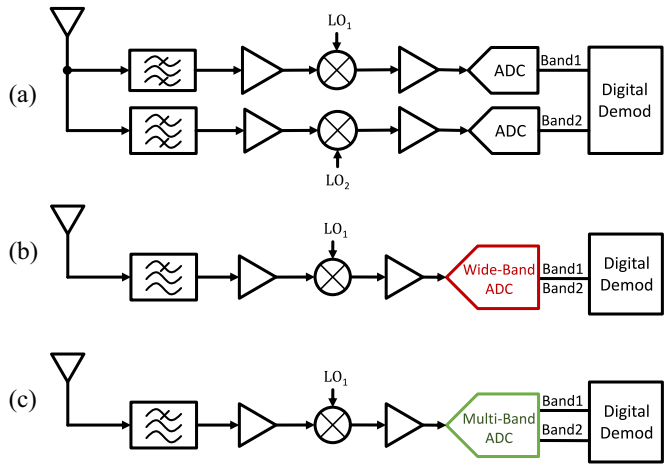

Fig. 1. (a) Conventional parallel receiver, (b) using power-hungry wide-band ADC, and (c) multiband CT-ΔΣ ADC reduces ADC power and simplifies front end.

II. Multiband Architecture

We begin with an overview of the architecture. Fig. 2(a) shows a conceptual representation of a two-band ΔΣ modulator. In this letter, the BB is third-order, and the bandpass (BP) is sixth-order, resulting in a ninth-order loop, overall. In the loop filter of Fig. 2(a), FF paths bypass each band's subfilter. This isolates the bands from one another, keeping each from having to process the other's noise in addition to its own. Instead, the noise is passed through resistive FF paths which do not have the linearity and bandwidth limitations of the subfilters.

Fig. 2(b) shows the fully realized prototype, in which each subfilter is synthesized as a cascade of biquads using the method introduced in Section III. Each filter block is a single biquad with two poles and one zero. Since summations are implemented in current mode, with the FF resistors feeding into the following biquad's virtual ground, the output of these summations cannot be accessed directly to implement an FF. As a result, FF paths f_1 and f_2 must be split up into new FF paths to make an equivalent, implementable signal flow, shown with coefficients f_2, $f_2 * b_1$, and $f_1 * f_2$ in Fig. 2(b). The NRZ DACs and quantizer are both 12-level and the sampling rate is fixed at 2 GHz. The final summation before the quantizer is implemented using a transimpedance amplifier (TIA). The CT delays are passive all-pass filters and are discussed in Section V.

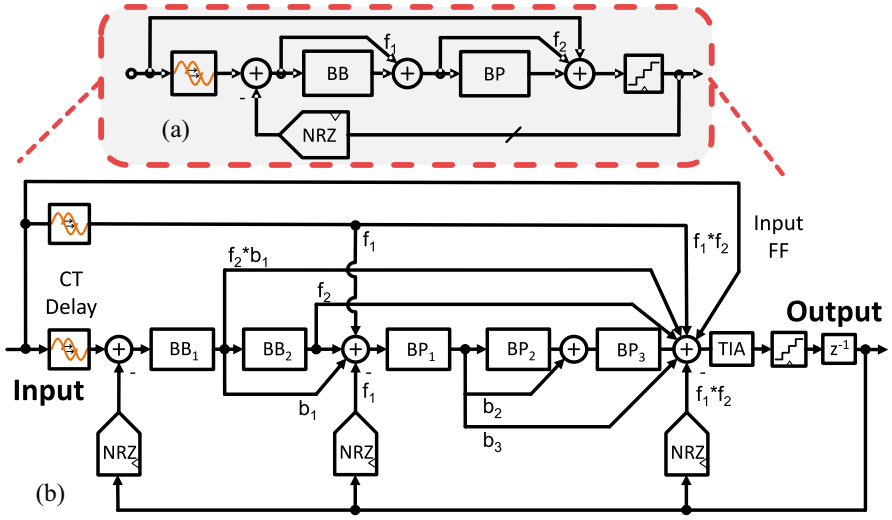

Fig. 2. (a) Conceptual overview and (b) detailed block diagram of the modulator. In (a), BB and BP blocks are third- and sixth-order filters, respectively. In (b), BB_1 is an integrator, BB_2 and all BP blocks are single-amplifier biquads.

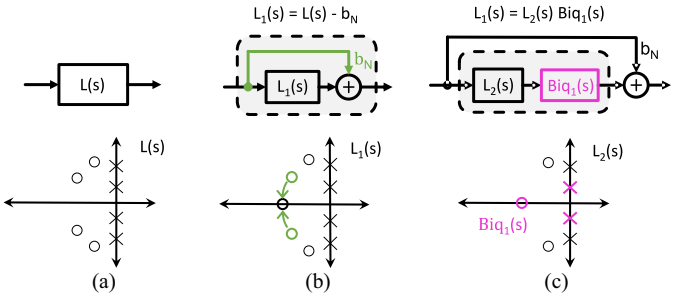

Fig. 3. FF synthesis method: (a) Required filter, (b) FF removed from $L(s)$, and (c) biquad (with 1 zero) factored from $L_1(s)$, then repeat (b) on $L_2(s)$ and so on.

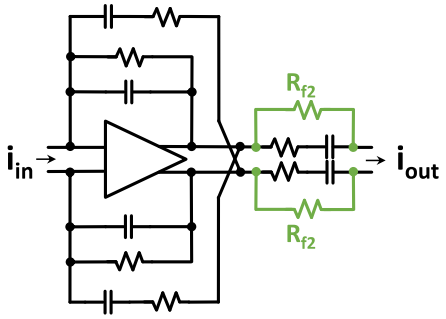

Fig. 4. Modified biquad; R_{f2} added.

III. Loop Filter Synthesis for Multiband Modulator

A challenge of the MB-$\Delta\Sigma$M is that the overall filter order is large because it combines lowpass and BP filter responses. High-order modulators are notoriously difficult to design; to address this, we adopt a cascaded form and introduce a new modulator synthesis technique.

The difficulty with high-order modulators is that most practical structures are not suited for high-order modulation due to a high sensitivity to small errors in the feedback and FF gains. Consider a CT version of the classic CRFF filter structure from [3]. When implementing a fourth-order transfer function, the open-loop denominator is: $s^4 + (g_1 + g_2)s^2 + g_1 g_2$, with local feedback paths g_1 and g_2. While there are many benefits to this architecture, it does not scale well with order: the roots of some high-order polynomials become more sensitive to small perturbations in their coefficients [4], meaning the open-loop pole locations become equally sensitive to the gain of the feedback paths g_1 and g_2. To alleviate this problem, we implement the filter in a cascaded form by constructing each pair of poles and zeros using biquads. While the use of biquads in a CT-$\Delta\Sigma$ modulator is not unusual, it is critical to successfully designing very high-order modulators.

In order to design the complex loop filter required for a multiband modulator, we develop a synthesis method to iteratively produce the filter from the desired response. Our process (Fig. 3) is inspired by the passive filter synthesis technique in [5] and facilitates efficient single-opamp biquads [6] which are limited to two poles and a single zero. Consider the desired transfer function, $L(s)$, shown in Fig. 3(a). If the transfer function has an equal number of poles and zeros, then subtracting a constant removes the leading term in the numerator by cancelling its coefficient. It can be said that we have "removed" a zero, since the numerator of the remainder, $L_1(s)$, is now one degree less. This subtraction of a constant can be implemented as an FF path around $L_1(s)$, shown in Fig. 3(b). We can now implement (i.e., "remove") two of $L_1(s)$'s poles and the (real) zero that has been created using a biquad and we are left, again, with a transfer function having an equal number of poles and zeros, $L_2(s)$, shown in Fig. 3(c). The process is repeated until the last biquad is implemented and nothing remains. This filter design process can be easily applied to any desired loop filter, regardless of its complexity.

IV. Modified Single-Amplifier Biquad

We implement the poles and zeros for each individual section using a modified version of the single-amplifier biquad in [6], shown in Fig. 4. A drawback of [6] is that it requires a complex system of DACs to stabilize the modulator due to insufficient freedom in the placement of zeros. We add an extra resistive path (R_{f2}) to the forward network, which adds a constant term in the numerator of the passive forward path's transfer function. This creates the extra degree of freedom needed for the biquad to implement any real zero. It alleviates the need for DACs with complex shapes, reducing power consumption, and simplifying the design process.

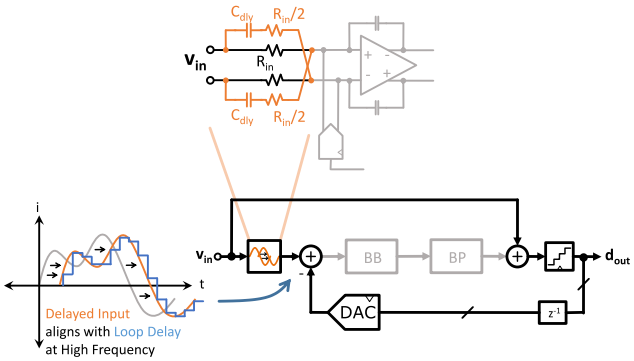

Fig. 5. Delay matching all-pass filter in the input network.

V. Improved Linearity Through Loop-Delay Matching

Digitizing multiple bands with the same ADC has the potential to cause significant interband distortion products. We apply and improve the conventional linearity-improving input FF technique [3] which allows the input signal to bypass the amplifiers through an input FF, as shown in Fig. 2(a). Since the FF path is injected just before the quantizer, any signal distortion from the FF path due to the TIA is noise-shaped, keeping the two bands well isolated from each other. However, for CT modulators, the conventional resistive FF cannot fully cancel the input at high frequencies due to the extra phase and gain induced by the TIA, loop delay, and DAC, limiting the linearity benefits. As shown in Fig. 5, fully canceling the input requires that the input signal and its replica, after traveling around the loop, be identical in both magnitude and phase. To approximate this, we add a first-order model of the loop delay to the input network by changing the input resistors into passive all-pass filters. This cross-coupled path adds a left-half-plane pole and right-half-plane zero at the same frequency, set by C_{dly}. The pole and zero cancel each other's magnitude but add 180 degrees of phase shift. The transition of this phase shift is chosen so that the phase of the input path within the BP region approximates the phase of the FF path as it returns to the input summing node. This new approach requires only simple modifications to the existing resistive input and reduces the input signal present in the high-frequency biquads by >10 dB over the BP bandwidth.

VI. Noise-Shaping Budget

Multiband noise-shaping is a specific instance of the more general concept of arbitrary noise-shaping, wherein any desired NTF can be realized. The "noise-shaping budget," then, is a simple way to compare the efficiency of one arbitrary modulator to another. According to the Bode sensitivity integral

$$\int_{\omega} \log |\mathrm{NTF}(z)| dz = 0 \tag{1}$$

where the integration path, ω, is the unit circle. Put simply: the integral of the NTF's magnitude, in dB, must be 0. That is, any noise removed from one area of the spectrum must be balanced by an increase in a different area [3]. However, Lee's rule requires that the maximum gain at all frequencies be less than a constant (which depends on the quantizer precision) for the modulator to remain stable.

This implies the concept of a noise-shaping budget: the maximum amount of noise-shaping—defined as the out-of-band portion of the sensitivity integral in (1)—depends only on the quantizer, which sets the maximum NTF gain (i.e., Lee's rule), and the modulator's order,

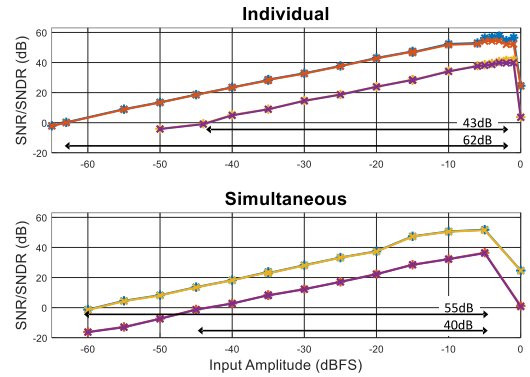

Fig. 6. Measured SNDR versus input amplitude for single-band and multiband operation. In (top), blue and orange represent SNR and SNDR for the BB; purple and gold for BP. In (bottom), yellow and teal are for the BB; purple and orange for the BP. In the multiband case, all measurements at each input amplitude are taken simultaneously.

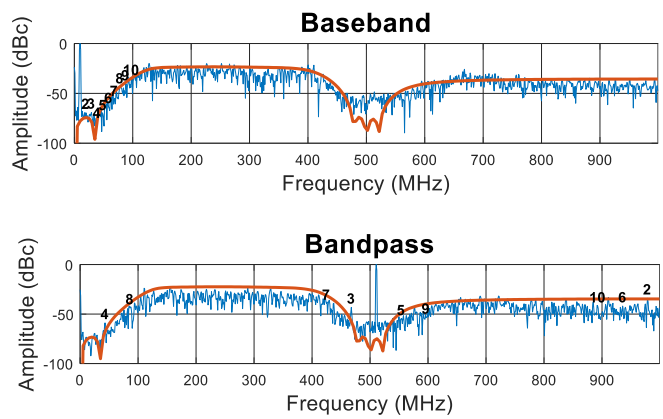

Fig. 7. Measured spectra for each single-band operation.

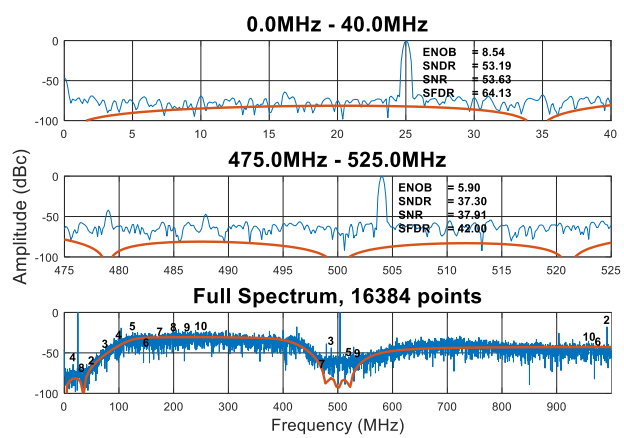

Fig. 8. Measured spectrum for multiband operation: (top) BB only, (middle) BP only, and (bottom) full spectrum.

which changes the slope of the transition between in-band and out-of-band regions. There is no restriction on noise-shaping and, therefore, it may be distributed as-needed throughout the spectrum. This concept is what makes multiband noise-shaping possible and, though this letter demonstrates a 2-band modulator, any configuration of bands meeting the given budget is possible.

Note that the noise-shaping budget also implies the sample-rate and quantizer requirements can be roughly estimated using

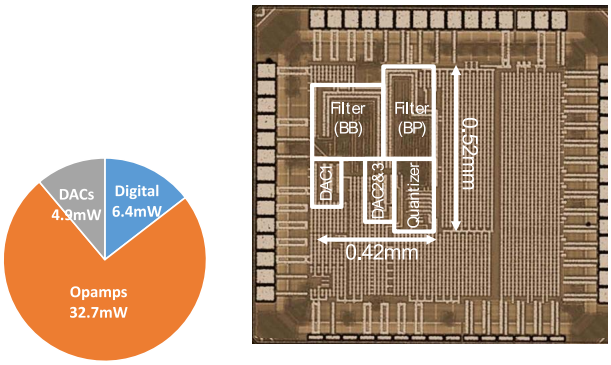

Fig. 9. Power breakdown and die photograph of the MB-ΔΣM.

existing single-band techniques and fine-tuned by accounting for the extra transition-bands required and through simulations.

VII. Measurement Results

The prototype is fabricated in 40-nm CMOS, occupies 0.22 mm^2 and consumes 45 mW from a 1.2-V supply. Shown in Fig. 6, the measured dynamic range (DR) is 62 dB in the BB and 43 dB in the BP. Fig. 7 shows the measured spectra for a single tone in each band, demonstrating a peak SNDR of 54.3 dB and 41.4 dB for 10 MHz and 504 MHz inputs, respectively. Fig. 8 shows the spectrum for simultaneous tones in both bands, demonstrating a peak SNDR of 55 and 39 dB or, at most, 2.4 dB less than with single-band operation. In this test, the tones are at equal power—after compensating for slight differences in measured STF—and are increased together until instability, using a worst-case choice of BP frequency; where the fourth and eighth BP harmonics fall in the BB. Note that the interband distortion tones do not contribute significantly to the BB SNDR. The SFDR in each band—including interband distortion components—is 64 dB and 42 dB, respectively.

Fig. 9 shows the power distribution and a die photo. The quantizer and digital buffers in the feedback path are included in the "Digital" category.

VIII. Conclusion

We present the first MB-ΔΣM. To realize this new architecture, we also: 1) develop an FF synthesis method that simplifies loop filter design; 2) develop a single-amplifier biquad that allows for simpler DAC design; and 3) reduce interband distortion through loop-delay matching. By saving significant power both in the RF front end and through its efficient use of the noise spectrum, the MB-ΔΣM is an enabling technology for interband CA in emerging wireless standards.

Finally, by demonstrating that arbitrary noise-shaping is possible, this letter is a step toward custom, application-driven noise-shaping solutions that provide new tools to solve difficult design problems. While this prototype is an important first step, the future work must demonstrate the addition of more than 2-bands, tunability of band separations, and must more precisely address the needs of specific application areas, such as LTE and 5G.

References

[1] R. Chen and H. Hashemi, "Reconfigurable SDR receiver with enhanced front-end frequency selectivity suitable for intra-band and inter-band carrier aggregation," in *Proc. IEEE Int. Solid-State Circuits Conf. (ISSCC)*, 2015, pp. 1–3.

[2] Y. Dong *et al.*, "A 930mW 69dB-DR 465MHz-BW CT 1-2 MASH ADC in 28nm CMOS," in *Proc. IEEE Int. Solid-State Circuits Conf. (ISSCC)*, 2016, pp. 278–279.

[3] S. Pavan, R. Schreier, and G. C. Temes, *Understanding ΔΣ Data Converters*. Piscataway, NJ, USA: IEEE Press, 2017.

[4] J. H. Wilkinson, *Studies in Numerical Analysis*. Washington, DC, USA: Math. Assoc. America, 1984.

[5] W.-K. Chen, *Passive, Active, and Digital Filters*. Boca Raton, FL, USA: Taylor & Francis, 2006.

[6] J. Jeong, N. Collins, and M. P. Flynn, "A 260 MHz IF sampling bit-stream processing digital beamformer with an integrated array of continuous-time band-pass ΔΣ modulators," *IEEE J. Solid-State Circuits*, vol. 51, no. 5, pp. 1168–1176, May 2016.